Translational Oncology 14 (2021) 101109

Contents lists available at ScienceDirect

Translational Oncology

journal homepage: www.elsevier.com/locate/tranon

Original Research

A novel tailored immune gene pairs signature for overall survival prediction in lower-grade gliomas

Xuyan Pan[a,1], Zhaopeng Wang[b,1], Fang Liu[b], Feihui Zou[b], Qijun Xie[b], Yizhuo Guo[b], Liang Shen[b,*]

[a] Department of Neurosurgery, Huzhou Cent Hospital, Affiliated Cent Hospital Huzhou University, 1558 Third Ring North Road, Huzhou, Zhejiang 313000, China
[b] Department of Neurosurgery, The affiliated Changzhou No.2 People's Hospital of Nanjing Medical University, 68 Gehu Road, Changzhou, Jiangsu 213000, China

ARTICLE INFO

Keywords:
Lower-grade gliomas
Immune
Weighted gene co-expression network analysis
Nomogram
Prognosis

ABSTRACT

Lower-grade gliomas (LGGs) have a good prognosis with a wide range of overall survival (OS) outcomes. An accurate prognostic system can better predict survival time. An RNA-Sequencing (RNA-seq) prognostic signature showed a better predictive power than clinical predictor models. A signature constructed using gene pairs can transcend changes from biological heterogeneity, technical biases, and different measurement platforms. RNA-seq coupled with corresponding clinical information were extracted from The Cancer Genome Atlas (TCGA) and the Chinese Glioma Genome Atlas (CGGA). Immune-related gene pairs (IRGPs) were used to establish a prognostic signature through univariate and multivariate Cox proportional hazards regression. Weighted gene co-expression network analysis (WGCNA) was used to evaluate module eigengenes correlating with immune cell infiltration and to construct gene co-expression networks. Samples in the training and testing cohorts were dichotomized into high- and low-risk groups. Risk score was identified as an independent predictor, and exhibited a closed relationship with prognosis. WGCNA presented a gene set that was positively correlated with age, WHO grade, isocitrate dehydrogenase (IDH) mutation status, 1p/19 codeletion, risk score, and immune cell infiltrations (CD4 T cells, B cells, dendritic cells, and macrophages). A nomogram comprising of age, WHO grade, 1p/19q codeletion, and three gene pairs (BIRC5|SSTR2, BMP2|TNFRSF12A, and NRG3|TGFB2) was established as a tool for predicting OS. The IPGPs signature, which is associated with immune cell infiltration, is a novel tailored tool for individual-level prediction.

Introduction

Glioma, the most common malignant brain tumor, derives from glial or neural stem cells. Glial cells surround and support the neurons, transmitting electric and chemical signals in the central nervous system. The World Health Organization (WHO) classification grades glioma from I–IV based on the extent of glioma cell resemblance to normal cells, mitotic activity, microvascular proliferation, and necrosis among others. The 2016 WHO classification is more scientific in grading as it considered the status of some molecular markers [1]. WHO grade I glioma cells correspond to well-differentiated glial tumors, whereas WHO grade II and III, together, are together known as lower-grade glioma. WHO grade IV includes two types of glioblastoma (GBM): Secondary GBM originating from lower-grade glioma and primary GBM [2]. Glioma symptoms vary depending on tumor location and size. Common symptoms are seizures, headaches, limb weakness, speech problems, and memory loss.

Therapeutic options for glioma are continuously being evaluated and novel surgical procedures are gradually being advanced. For example, awake craniotomy and intraoperative imaging aids in the identification of tumor boundaries and key brain areas, thereby enhancing tumor resection while preventing nerve function deficits [3,4]. However, despite advances in therapy, glioma prognosis is still poor and unpredictable. The prognosis of lower-grade glioma is better than that of GBM, with better survival outcomes. Therefore, a risk assessment tool for prognostic prediction of lower-grade glioma may be beneficial. However, concordance of different clinical criteria for risk stratification is low as clinical trials using clinical factors (age, tumor diameter, and whether the tumor crosses the midline among others) are not comparable [5]. Therefore, a unified risk management for survival prediction is necessary. Various survival predictive signatures using RNA sequences have been shown to be powerful survival prediction tools [6–10]. Survival predictive signatures can be used to create novel and innovative clinical indicators to improve the concordance of different criteria.

* Corresponding author.
E-mail address: soochowneuro@163.com (L. Shen).
[1] Xuyan Pan and Zhaopeng Wang should be considered joint first author.

https://doi.org/10.1016/j.tranon.2021.101109
Received 9 February 2021; Received in revised form 26 March 2021; Accepted 16 April 2021

Most therapeutic options for gliomas have limited efficacies. Novel immunostimulatory strategies attract more attention due to their sensitive anti-glioma responses compared to conventional therapies [11]. Genomic studies have revealed the immunological mechanisms of glioma growth, leading to the identification for glioma immune checkpoints [6,12]. The tumor immune risk stratification management is important for elucidating immunotherapeutic mechanisms. A simple and feasible individualized prognostic signature has a more valuable function in clinical trials. However, practical applications of predictive signatures are limited. This is because differences in measurement platforms affect sample homogenization, making the sample risk score to become cumbersome and unstable. If references were from a single sample, defects from the prognostic predictive system caused by high biological heterogeneities, technical biases, and different measurement platforms, would be overcome. Fortunately, gene pairs based on relative expression levels between two genes can transcend these challenges [13]. This study presents an immune gene pair signature established using machine learning. It can be used for individual OS predictions for glioma patients. Resource can be saved accurate predictive signatures for prognosis.

Material and methods

Identification of immune-related gene pairs

RNA-sequence data, and the corresponding clinical information in the prognostic signature were download from the Cancer Genome Atlas (TCGA) (https://portal.gdc.cancer.gov/) and the Chinese Glioma Genome Atlas (CGGA) (http://www.cgga.org.cn/). Samples with missing clinical data, including age, sex, IDH mutation status, survival time, or with survival time < 90 days were excluded. Differences in clinical characteristics was analyzed by SPSS (Version 20). $p < 0.05$ was set as the threshold for statistical significance. The gene set with immune-related genes was identified using the IMMPORT website (https://www.immport.org/). Samples in TCGA were assigned to the training cohort, whereas samples in CGGA were assigned to the testing cohort.

Establishment and validation of the prognostic signature

Immune-related prognostic genes with $p < 0.05$ identified using Cox regression analysis and Kaplan-Meier (KM) survival analysis in TCGA and CGGA were separately screened. Then, these genes were used to intersect to obtain a new gene set. Probably, immune-related gene pairs (IRGPs) had a natural advantage, thereby eliminating the necessity for normalization in individual prognostic analysis. IRGPs were defined through pair-wise comparisons based on gene expression levels in the same sample [13]. The IRGPs were scored as "1″ if the expressions were IRG1>IRG2, otherwise, they would "0″. In two special cases, the IRGPs were calculated as 0 and 1, and were excluded to reduce bias or avoid unrepeatability. Univariate and multivariate Cox proportional hazards regression analyses were performed to establish a prognostic model. The risk score for each sample was calculated using the model formula [6]. The optimal cut-off value of the 3-year area under the curve (AUC) was identified as the point at which the sum of specificity and sensitivity was maximal. Then, samples were assigned into groups of two for further analyses.

Validation of the prognostic signature

External and internal verification were used to evaluate the predictive ability of the signature. Two KM survival curves for OS were first compared using the log-rank test ($p < 0.05$) [14], while the 1-, 3-, and 5-year time-dependent receiver operating characteristic (ROC) curves were visualized in the training and testing cohorts [15]. The risk score coupled with five clinical factors (age, sex, WHO grade, IDH mutation status, and 1p/19q codeletion status) was tested for independent assessment using univariate and multivariate Cox regression analyses. Principal component analysis (PCA), a publicly known source apportionment method, was performed for hierarchical clustering [16–18].

Establishment and validation of the nomogram

A nomogram for survival prediction was established based on the prognostic factors, and was validated in the testing cohort. A calibration curve plot was used to validate the predictive accuracy and the concordance index [19,20]. Net reclassification index (NRI) [21], combined with decision curve analysis (DCA) [22] were performed to choosing select an optimized signature. The source of the prognostic signature was transferred to a webpage, shiny (https://shiny.rstudio.com/), using the "DynNom" R package, which makes it easy for users to predict individual prognosis.

Risk score immune cell infiltration

To establish a landscape of risk scores and infiltrating immune cells, infiltration intensity was assessed through the web app, Immune Cell Abundance Identifier (immuneCellAI), by uploading the LGG RNA-seq data [23]. Differential distributions of 24 types of immune cells between the low-risk and high-risk groups were visualized. Moreover, differential expression levels of six established immune checkpoint genes (CD48, CD274, cytotoxic T lymphocyte antigen 4 (CTLA4), T cell immunoglobulin domain and mucin domain 3 (TIM3), long non-coding RNA MIR 155 host gene (MIR155HG), and programmed cell death 1 (PD1)) in the high-risk and low-risk groups were analyzed ($p < 0.05$).

Weighted gene co-expression network analysis (WGCNA)

WGCNA, firstly proposed by Zhang and Horvath [24], is a powerful tool for evaluating correlations among genes by assigning a connection weight. Compare to traditional methods, it is biologically meaningful [25,26]. The top 25% variant median absolute deviation sample were screened for WGCNA. Sample clustering was performed to detect outliers in the data, and to reduce the impact of heterogeneity. The best-correlated relationship between the WGCNA module and biological traits (including IDH mutation status, 1p/19q codeletions status, CD4 T cells, B cells, and dendritic cells, macrophage among others) was selected for biological processes analyses. The network was developed through co-expression relationships that were achieved using WGCNA and visualized in Cytoscape v3.7.0 [27].

Gene ontology analysis

GO analysis is a biological method for evaluating the mechanisms involved in three domains: biological process (BP), cellular component (CC), and molecular functions (MF). Hub genes with a weight larger than 0.20 in the target module were screened using GO analysis to evaluate module function in WGCNA.

Results

Prognostic signature establishment

A total of 298 immune genes that were screened from the TCGA were associated with overall survival outcomes, 44 of which were identified as intersecting genes in CGGA. Eight pair-wise immune genes were extracted for establishing the prognostic signature (Table 1). The preferable cutoff value for distinguishing the high-risk group ($n = 100$) and low-risk group ($n = 359$) in the TCGA was −0.145 (**Fig. 1a,c**). Similarly, a total of 118 samples were defined as high-risk while 414 samples were involved in the low-risk set in CGGA. A total of 449 samples in TCGA and 459 samples in CGGA were finally included by excluding the samples without clinical indication (Table 2).

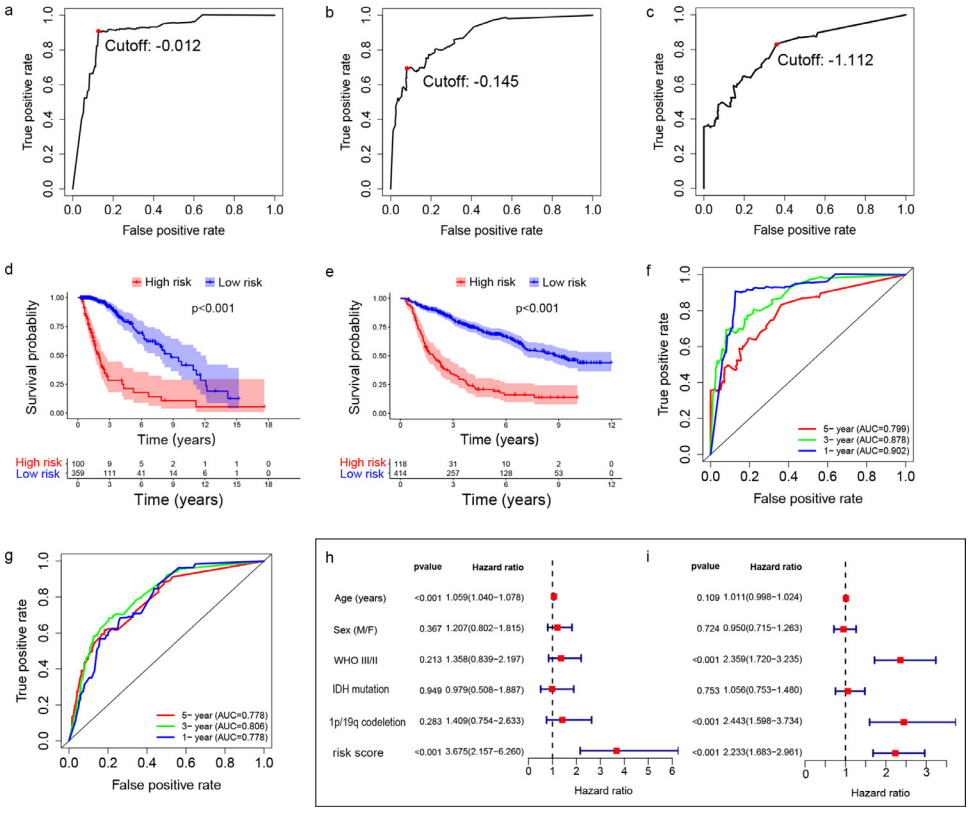

Fig. 1. The cut-off value of 1-year (a), 3-year (b), and 5-year (c) AUCs. The cut-off value of 3-year AUC was the optimal value for grouping. Kaplan-Meier (KM) survival curves illustrate that the prognosis of the low-risk group was more favorable in the training group (d), as well as in the testing group (e). The time-dependent receiver operating characteristic (ROC) curves for the 1-, 3- and 5-year survival rates in training group (f) and testing group (g). Risk score is an independent survival predictor of age, sex, WHO grade, IDH mutation status, and 1p/19q codeletion status in univariate (h) and multivariate Cox proportional hazards regression analyses (i).

Table 1
Eight gene pairs and coefficients in the prognostic signature.

Gene Pairs	Coef	Gene Pairs	Coef
PDIA2|WNT5A	−0.097987276	PDIA2|SLC11A1	−0.044735657
LCNL1|CTF1	−0.056923104	MSR1|CHGA	0.004112451
BIRC5|SSTR2	0.42711727	BMP2|TGFB2	−0.014125758
BMP2|TNFRSF12A	−0.460456827	NRG3|TGFB2	−0.54034719

PDIA2: protein disulfide isomerase family A member 2, WNT5A: Wnt family member 5A, LCNL1: lipocalin like 1, CTF1:cardiotrophin 1, SSTR2:somatostatin receptor 2, BIRC5:baculoviral IAP repeat containing 5, BMP2: bone morphogenetic protein 2, TNFRSF12A:TNF receptor superfamily member 12A, MSR1:macrophage scavenger receptor 1, TNFRSF12A:TNF receptor superfamily member 12A, SLC11A1: solute carrier family 11 member 1, CHGA: chromogranin A, TGFB2:transforming growth factor beta 2, BMP2:bone morphogenetic protein 2, BIRC5: baculoviral IAP repeat containing 5.

Table 2
The clinical characteristics of included samples in TCGA and CGGA.

Variables	TCGA (449)	CGGA (459)	Value	*P* value
Sex			1.056	0.034
Female	203	192		
Male	246	267		
Age (year)				
<40	203	221	0.786	0.375
≥40	246	238		
OS (year, median)	6.67	6.85	2.583	0.108
Histology type			121.030	<0.001
Astrocytoma	148	150		
Oligodendroglioma	146	77		
Oligoastrocytomas	104	232		
NA	51	0		
WHO grade			0.014	0.096
WHO II	215	218		
WHO III	234	241		
IDH mutation			5.645	0.018
Yes	364	342		
No	85	117		
1p/19 codeletion			0.504	0.478
Yes	309	319		
No	150	140		

NA: Not available.

Survival prediction assessment and validation

The survival rate of the low-risk group was higher than that of the high-risk group for the training (Fig. 1**d**) and testing cohorts (Fig. 1**e**), especially in the definite period of the early course of the disease. AUC values of the signature for 1-, 3-, and 5-year were 0.902, 0.878, and 0.799, respectively. In the testing cohort, AUC values of 1-, 3-, and 5-year were 0.778, 0.806, and 0.778 respectively, indicating an accurate prediction from the signature (Fig. 1**f,g**). The risk score was a definite prognostic factor that was independent of age, sex, WHO grade classification, IDH mutation status, and 1p/19q codeletion status, both in the training and testing cohorts (Fig. 1**h,i**).

Contribution of the signature to immune status

Distribution patterns of all the genes, as well as immune-related genes in the TCGA and intersecting immune-related genes in CGGA, were analyzed using three-dimensional principal component analysis (PCA). Compared to the immune-related genes set (Fig. 2b) and all the other genes set (Fig. 2c), it was found that the intersecting immune-related genes involved in signature establishment (Fig. 2**a**) could be used to divide the samples into low-risk and high-risk groups. The correlation between risk score and immune cell infiltrations is presented in the violin plot. Seventy-five percent (18/24) of the immune cells exhibited a positive or negative correlation with the risk score ($p < 0.05$) (Fig. 2**d**). Significant immune cells in the plot include innate immune cells such as macrophages and DC cells as well as adaptive immune cells such as B

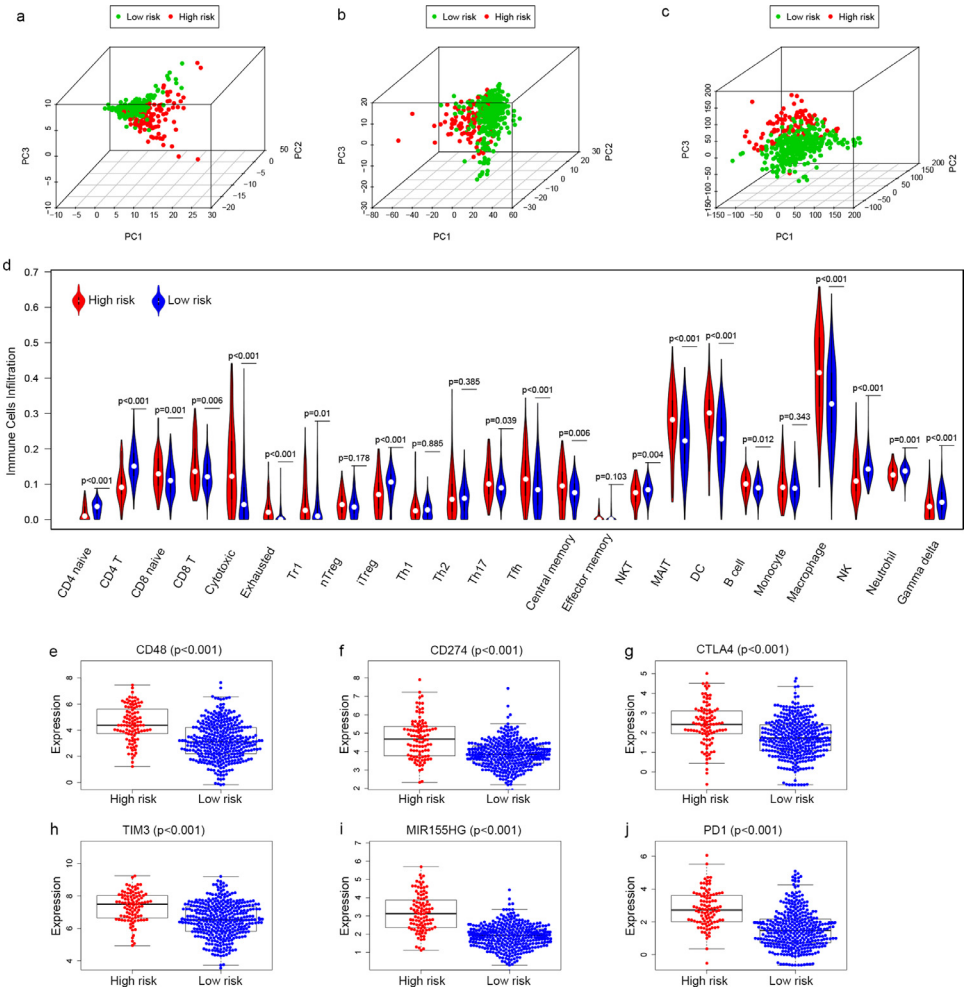

Fig. 2. The PCAs of intersecting immune-related genes set (a), immune-related genes set (b), and all genes set (c) in the low and high-risk groups. Twenty-four kinds of immune cells infiltration in the low and high-risk group (d). The expression of six kinds of immune checkpoints in the low and high-risk groups (e–j).

cells and CD4 T cells. Expression levels of six immune checkpoint genes (CD48, CD274, CTLA4, TIM3, MIR155HG, and PD1) were higher in the high-risk group than in the low-risk group (Fig. 2**e-j**).

Gene co-expression network and hub genes

Hierarchical clustering and Dynamic Branch Cutting clustered the genes into 13 modules representing different gene sets with varying sizes from 57 to 965 genes (**Fig. 3a**). The correlation between module eigengenes and risk score, macrophages, DC cells, B cells, and CD4 T cells, was used to establish a discriminatory module for prognostic mechanisms. In **Fig. 3b**, the yellow module is bound with the risk score; macrophages, DC cells, B cells, and CD4 T cells have the highest module membership (MM) than other modules. The gene co-expression network was established based on the hub genes whose weight was >0.20 (Supplement material 1). In the complicated co-expression network constructed using 87 genes from the yellow module, most of the genes were found to be differential expression genes (DEGs) with a $|\log2FC| > 0.6$ between the high-risk and low-risk groups (**Fig. 4**). Moreover, 65 (65/87) genes were correlated with OS. Therefore, a new gene set comprising 87 hub genes was used for GO enrichment analyses. The hub genes were enriched in immune-related functions, such as neutrophil activation, and neutrophil degranulation, neutrophil-mediated immunity among others (**Fig. 5**). More GO functions can be found in the Supplement material 2.

Optimization of the prognostic model

Three gene pairs (BIRC5|SSTR2, BMP2|TNFRSF12A, NRG3|TGFB2) accounted for the vast majority of the proportions when calculating the risk score by comparing coefficients of the eight pairs of immune-related genes. Two models were built in this study. Model A, comprising age, WHO grade, 1p/19q codeletion status, IDH mutation status, as well as risk score and Model B comprising age, WHO grade, 1p/19q codeletion status, BIRC5|SSTR2, BMP2|TNFRSF12A, NRG3|TGFB2. Model B was progressive with fewer ingredients than model A. The 4-year NRI indicated that the predictive ability of model A was better, with 16.2% improvement, whereas the NRIs of 1-, 2-, 3-, 5- and 6-year were not significantly different between model A and B (Table 3). DCA curves indicated that prognostic models had better predictive abilities within a certain survival rate range, and prognostic assessment abilities between model A and model B were almost the same (**Fig. 6**).

Table 3
The NRI of risk-prediction in model A and B.

Year	NRI	95%CI Lower	Upper	Year	NRI	95%CI Lower	Upper
1	−0.020	−0.104	0.010	2	−0.067	−0.201	0.042
3	−0.160	−0.314	0.018	4	−0.162	−0.289	−0.044
5	−0.174	−0.400	0.007	6	−0.193	−0.462	0.024

NRI: Net reclassification index, CI: confidence intervals.

Nomogram establishment and validation

Six ingredients, including age, WHO grade, 1p/19q codeletion, BIRC5|SSTR2, BMP2|TNFRSF12A, and NRG3|TGFB2 were selected to establish the nomogram for predicting the 1-, 3-, and 5-year survival rates (**Fig. 7a**). The C-index of the Cox model was 0.874,

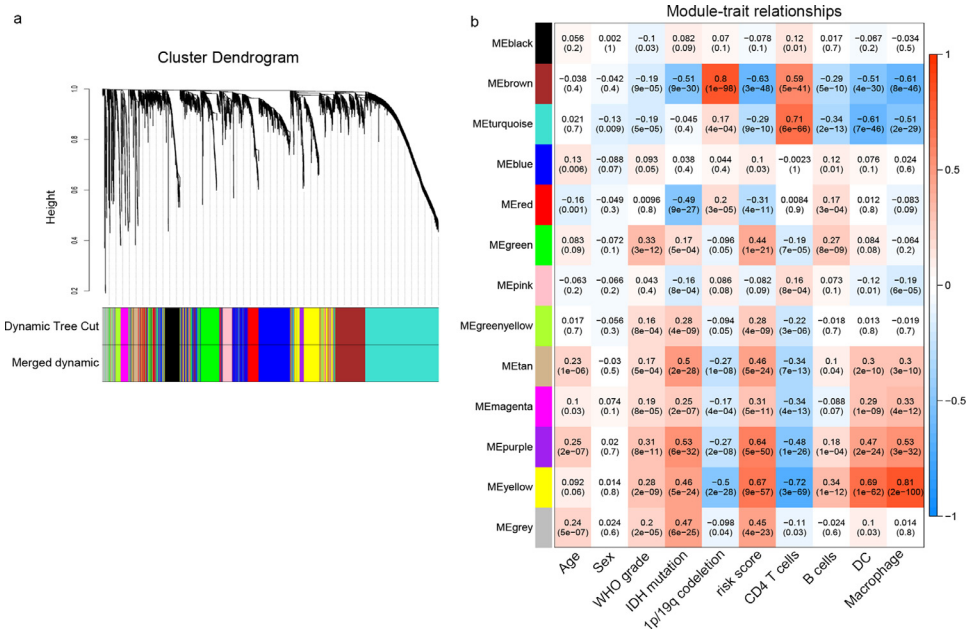

Fig. 3. The cluster dendrogram of genes in different models assigned with corresponding colors by dissimilarity based on topological overlap (a). Each rectangle, the intersection of module eigengene in the row and clinical predictors (age, sex, WHO grade, IDH mutation, 1p/19q codeletion) coupled with risk score and 3 kinds of immune cell infiltration in the column, contains a correlation and a *p*-value (b).

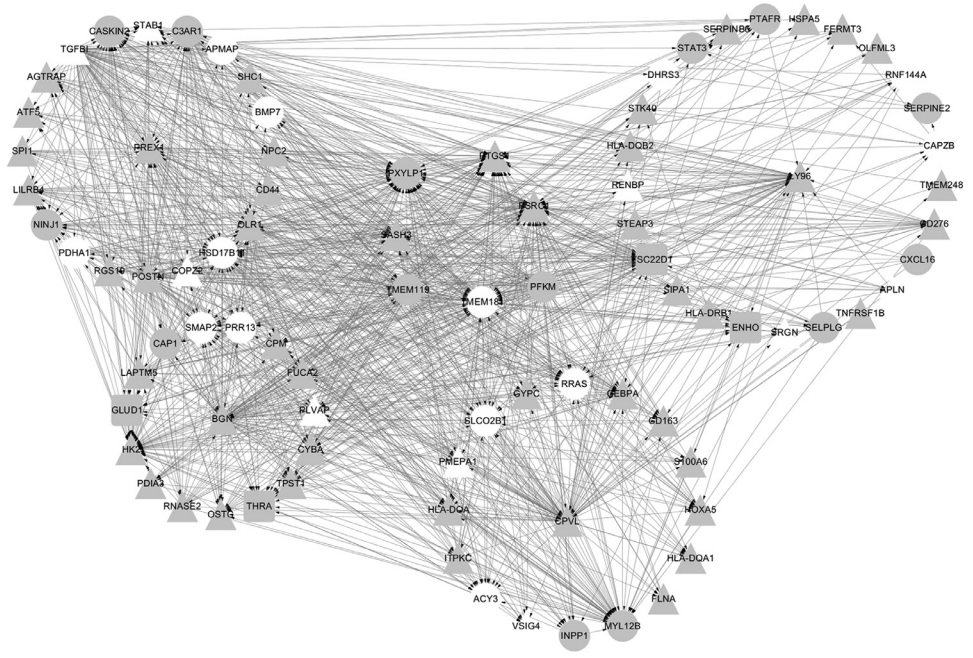

Fig. 4. The 87 genes constructed the gene network from the yellow module. Among the 87 genes, 56 (triangle) are highly expressed in the high-risk group, 4 (rectangle) are highly expressed in the low-risk group, and 27 (circle) have no difference in expression. Survival analysis indicated that 65 genes (gray) were related to OS with a p-value <0.05, the other genes (white) showed no relation to OS.

and the calibration curves of 1-, 3- and 5-year had goodness-off-fit (**Fig. 7b–f**). Web applications of our signature can be access to https://soochowneuro.shinyapps.io/immunepairB/?_ga=2.184366244.349859851.1606627026–2101425941.1599397013 for predicting the OS.

Discussion

The criteria proposed by the Radiation Therapy Oncology Group (RTOC) and the European Organization for Research and Treatment of Cancer (EORTC) were useful for predicting the prognosis of low-grade glioma [28,29]. However, Franceschi et al. [5] insisted that the criteria were not comparable due to poor concordance between RTOC and EORTC. As such, these two criteria are not as strong as expected. We propose an IRGPs prognostic signature that can decrease the effects of inherent biological sample heterogeneity, differences in measurement platforms, and technical bias, but may utilize more probable immunological mechanisms to improve the prognosis. Cox proportional hazards regression analyses were used to create a new analogous clinical prognostic predictor called “risk score”. The WGCNA provided new insights by integrating gene sets, clinical factors, and immune cell infiltration.

Clinical applications of traditional prognostic signatures are limited because of the differences in biological heterogeneity and laboratory technologies. A gene pair is a remodeling that quantifies the expression of two genes from the same sample with the same laboratory conditions. Gene pair is an expression of the targeted and reference genes from the one sample. Signatures that resemble gene pairs have been used in prognostic evaluations of various cancers [30–33]. Moreover, the concordance between the 1p/19 codeletion-associated immune prognostic signature developed in our earlier study [6] and the current gene pairs

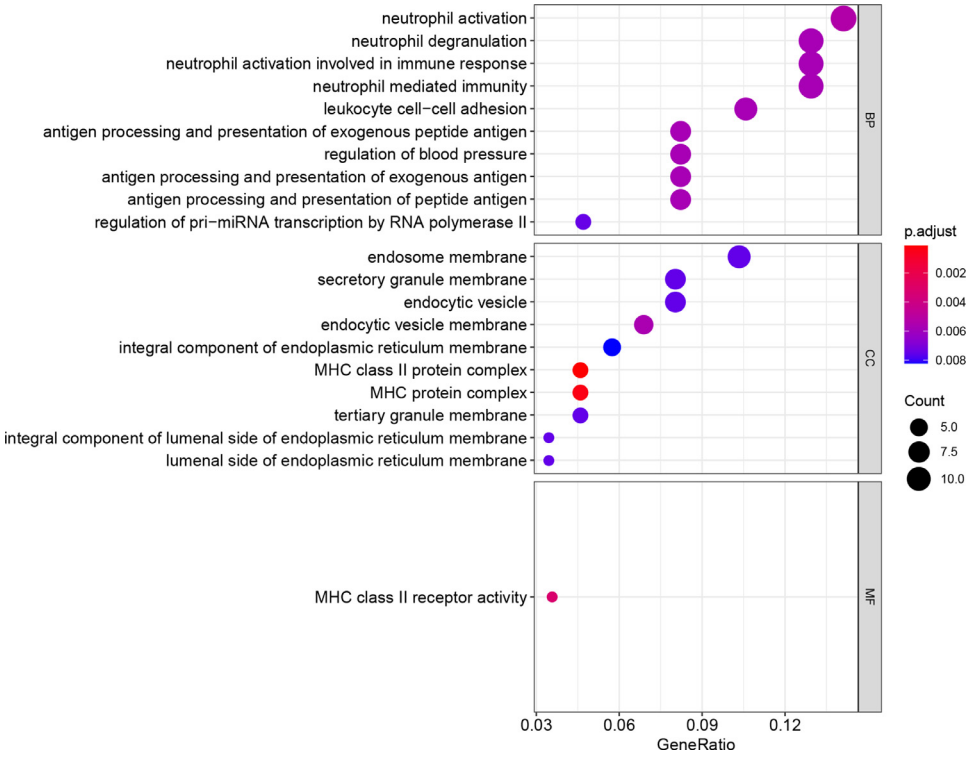

Fig. 5. GO analysis to the 87 DEGs between high-risk group and low-risk group shows the top 10 listed biological functions in BP, CC, and MF.

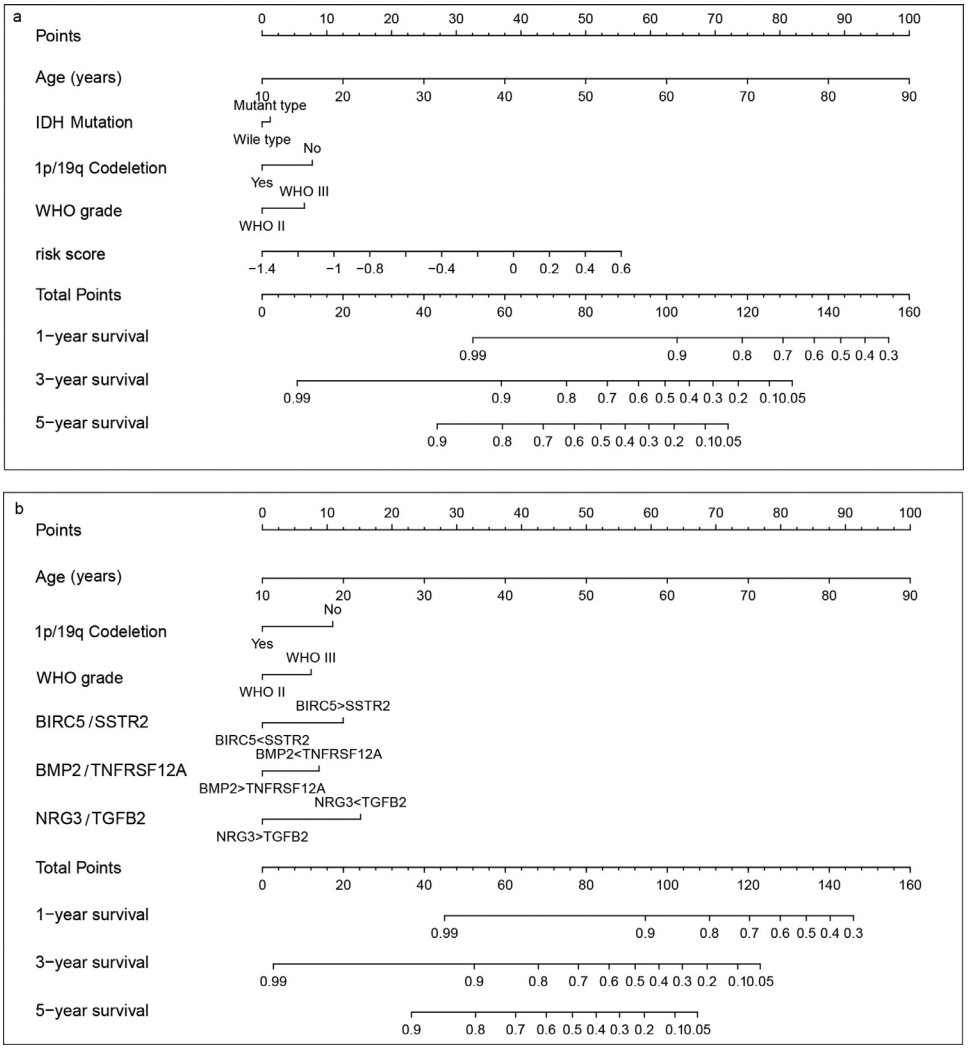

Fig. 6. The model A shows that age, IDH mutation, 1p/19q codeletion, WHO grade, and risk score are included as reference factors from each variable axis. The sum values in the axis including five factors can predicted the 1-, 3-, and 5-year survival rates (a). Similar, the model B including age, WHO Grade, 1p/19q codeletion status, BIRC5|SSTR2, BMP2|TNFRSF12A, and NRG3|TGFB2 can predict the 1-, 3-, and 5-year survival rates (b).

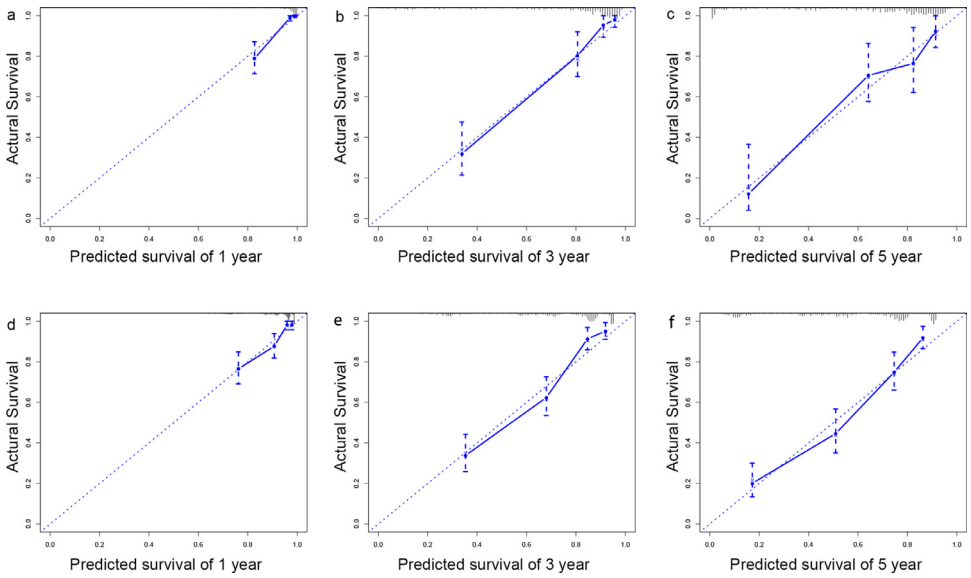

Fig. 7. Internal and external validation using calibration curves for predicting 1-, 3-, and 5-year survival in the TCGA (a,c) and CGGA (d,f).

signature was greatly improved than that of the EORTC and RTOG criteria [5]. We found that 93 (63.3%) glioma patients in the high-risk group of the 1p/19q codeletion-associated immune signature and 305 (97.8%) patients in the low-risk group met gene pairs signature criteria. Moreover, among the immune gene pairs signature high-risk patients ($n = 100$; 21.8%), 93 (93.0%) were scored as high risk, according to the 1p/19q codeletion-associated signature criteria. Among IRGPs signature low-risk patients ($n = 359$; 78.2%), 305 (85.0%) were scored as low risk according to the gene pairs signature criteria. Therefore, the IRGPs signature prediction of risk attribute is highly accurate. Coefficients in Table 1 show that three gene pairs (BIRC5|SSTR2, BMP2|TNFRSF12A, and NRG3|TGFB2) play a vital role in the establishment of risk score. The prognostic predictive ability of the simplified signature (model B), which included three gene pairs was similar to the original signature (model A) implying that model B is more economical without reducing performance.

Adaptive immune cells, for example, B cells and T cells, and innate immune cells including macrophages, neutrophils, and monocytes among others are the primary cancer immune response cells [23]. Many immune-associated gene signatures have been established and may imply that glioma prognosis is closely associated with the density of immune cell infiltrations [6,12,34,35], as well as laboratory studies [36,37]. However, most of the published signatures report differences in immune cell infiltrations in different risk stratifications of glioma. Rarely are further mechanisms described to identify cancer immunology. In this study, an IRGPs signature was first constructed, and WGCNA, a method proposed by Horvath et al. [24] to evaluate system-level biological meaning of genes [38], was used to determine a gene set correlated with immune cell infiltrations. The gene set in the yellow module is closely correlated with the established prognostic factors such as age, WHO grade, IDH mutation, and 1p/19 codeletion. The same gene set is highly correlated with immune cell infiltration that has been provided, playing a vital role in glioma prognosis [39,40]. Chai et al. [41] reported that neutrophils are biomarkers for regulating the prognosis of glioblastoma multiforme. GO enrichment analysis based on the DEGs in the high and low-risk groups, showed that immune-related functions, such as neutrophil activation involved in immune response, neutrophil-mediated immunity, occupy a dominant position. Moreover, CD48, CD274, CTLA4, TIM3, MIR155HG, and PD1, were identified as immune checkpoint genes [42–48]. Our findings imply that the signature may contribute to glioma immune risk stratification. More glioma prognostic mechanisms can be further evaluated by constructing a gene network.

This study elucidates on the available evaluation mechanisms for tumor microenvironment research studies associated with immunoregulation. Immune escape and immune therapy play a pivotal role in glioma growth. The IRGPs prognostic signature has more advantages than previous signatures. The signature is novel, but it is not flawless and the limitations should not be ignored. For example, tissue heterogeneity and tumor purity may silently affect individualized prognostic assessments. Single-cell sequencing may improve signature performance to a large extent. In addition, this signature is a temporary tool for predicant glioma prognosis, and studies should aim at advancing it.

Funding

This work was supported by the Youth Science and Technology Project of Changzhou (No.QN202034) and the Youth Program of Changzhou No. 2 People's Hospital (No. 2020K001).

Availability of data and material

The RNA-seq data and corresponding clinical information were observed from the TCGA (https://portal.gdc.cancer.gov/) and CGGA (http://www.cgga.org.cn).

Ethics approval

Not applicable.

Consent to participate

Not applicable.

Consent for publication

Not applicable.

Declaration of Competing Interest

The authors declare that they have no known competing financial interests or personal relationships that could have appeared to influence the work reported in this paper.

CRediT authorship contribution statement

Xuyan Pan: Data curation, Writing - original draft. **Zhaopeng Wang:** Data curation, Writing - original draft. **Fang Liu:** Supervision. **Feihui Zou:** Validation. **Qijun Xie:** Visualization. **Yizhuo Guo:** Writing - review & editing. **Liang Shen:** Conceptualization, Methodology, Software, Funding acquisition.

Acknowledgments

We would like to acknowledge the support of the Youth Science and Technology Project of Changzhou (No. QN202034) and the Youth Program of Changzhou No. 2 People's Hospital (No. 2020K001).

Supplementary materials

Supplementary material associated with this article can be found, in the online version, at doi:10.1016/j.tranon.2021.101109.

References

[1] P. Wesseling, D. Capper, WHO 2016 Classification of gliomas, Neuropathol Appl Neurobiol. 44 (2) (2018) 139–150, doi:10.1111/nan.12432.
[2] M. Kiran, A. Chatrath, X. Tang, D.M. Keenan, A. Dutta, A prognostic signature for lower grade gliomas based on expression of long non-coding RNAs, Mol. Neurobiol. 56 (7) (2019) 4786–4798, doi:10.1007/s12035-018-1416-y.
[3] O. Sacko, V. Lauwers-Cances, D. Brauge, M. Sesay, A. Brenner, F.E. Roux, Awake craniotomy vs. surgery under general anesthesia for resection of supratentorial lesions, Neurosurgery 68 (5) (2011) 1192–1198 discussion 1198-9, doi:10.1227/NEU.0b013e31820c02a3.
[4] R. Zelitzki, A. Korn, E. Arial, C. Ben-Harosh, Z. Ram, R. Grossman, Comparison of motor outcome in patients undergoing awake vs general anesthesia surgery for brain tumors located within or adjacent to the motor pathways, Neurosurgery 85 (3) (2019) e470–e476, doi:10.1093/neuros/nyz007.
[5] E. Franceschi, A. Mura, G. Lamberti, Biase D de, A. Tosoni, M. Di Battista, et al., Concordance between RTOG and EORTC prognostic criteria in low-grade gliomas, Future Oncol 15 (22) (2019) 2595–2601, doi:10.2217/fon-2019-0093.
[6] J. Xu, F. Liu, Y. Li, L. Shen, A 1p/19q codeletion-associated immune signature for predicting lower grade glioma prognosis, Cell Mol. Neurobiol. (2020), doi:10.1007/s10571-020-00959-3.
[7] B. Liu, J. Liu, K. Liu, H. Huang, Y. Li, X. Hu, et al., A prognostic signature of five pseudogenes for predicting lower-grade gliomas, Biomed. Pharmacother. 117 (2019) 109116, doi:10.1016/j.biopha.2019.109116.
[8] Z. Qian, Y. Li, X. Fan, C. Zhang, Y. Wang, T. Jiang, et al., Prognostic value of a microRNA signature as a novel biomarker in patients with lower-grade gliomas, J. Neurooncol. 137 (1) (2018) 127–137, doi:10.1007/s11060-017-2704-5.
[9] M. Zhang, K. Zhu, H. Pu, Z. Wang, H. Zhao, J. Zhang, et al., An immune-related signature predicts survival in patients with lung adenocarcinoma, Front. Oncol. 9 (2019) 1314, doi:10.3389/fonc.2019.01314.
[10] Y.Y. Zhao, S.H. Chen, Z. Hao, H.X. Zhu, Z.L. Xing, M.H. Li, A nomogram for predicting individual prognosis of patients with low-grade glioma, World Neurosurg. 130 (2019) e605–e612, doi:10.1016/j.wneu.2019.06.169.
[11] I.F. Parney, C. Hao, Petruk KC, Glioma immunology and immunotherapy, Neurosurgery 46 (4) (2000) 778–791 discussion 791-2., doi:10.1097/00006123-200004000-00002.
[12] X. Deng, D. Lin, B. Chen, X. Zhang, X. Xu, Z. Yang, Development and validation of an IDH1-associated immune prognostic signature for diffuse lower-grade glioma, Front. Oncol. 9 (2019) 1310, doi:10.3389/fonc.2019.01310.
[13] W. Chen, M. Ou, D. Tang, Y. Dai, W. Du, Identification and validation of immune-related gene prognostic signature for hepatocellular carcinoma, J. Immunol. Res. 2020 (2020) 5494858, doi:10.1155/2020/5494858.
[14] J.M. Reyes-González, B.I. Quiñones-Díaz, Y. Santana, P.M. Báez-Vega, D. Soto, F. Valiyeva, et al., Downstream effectors of ILK in cisplatin-resistant ovarian cancer, Cancers 12 (4) (2020) (Basel), doi:10.3390/cancers12040880.
[15] Z. Yang, J. Shang, N. Li, L. Zhang, T. Tang, G. Tian, et al., Development and validation of a 10-gene prognostic signature for acute myeloid leukaemia, J. Cell. Mol. Med. (2020), doi:10.1111/jcmm.15109.
[16] T. Konishi, S. Matsukuma, H. Fuji, D. Nakamura, N. Satou, K. Okano, Principal component analysis applied directly to sequence matrix, Sci. Rep. 9 (1) (2019) 19297, doi:10.1038/s41598-019-55253-0.
[17] P. Zhang, N.P. West, P.Y. Chen, M.W.C. Thang, G. Price, A.W. Cripps, et al., Selection of microbial biomarkers with genetic algorithm and principal component analysis, BMC Bioinf. 20 (Suppl 6) (2019) 413, doi:10.1186/s12859-019-3001-4.
[18] Z. Li, S.E. Safo, Q. Long, Incorporating biological information in sparse principal component analysis with application to genomic data, BMC Bioinf. 18 (1) (2017) 332, doi:10.1186/s12859-017-1740-7.
[19] K. Han, K. Song, Choi BW, How to develop, validate, and compare clinical prediction models involving radiological parameters: study design and statistical methods, Korean J. Radiol. 17 (3) (2016) 339–350, doi:10.3348/kjr.2016.17.3.339.
[20] G. Gandaglia, N. Fossati, E. Zaffuto, M. Bandini, P. Dell'Oglio, C.A. Bravi, et al., Development and internal validation of a novel model to identify the candidates for extended pelvic lymph node dissection in prostate cancer, Eur. Urol. 72 (4) (2017) 632–640, doi:10.1016/j.eururo.2017.03.049.
[21] M.B. Mortensen, V. Fuster, P. Muntendam, R. Mehran, U. Baber, S. Sartori, et al., Negative risk markers for cardiovascular events in the elderly, J. Am. Coll. Cardiol. 74 (1) (2019) 1–11, doi:10.1016/j.jacc.2019.04.049.
[22] B. van Calster, L. Wynants, J.F.M. Verbeek, J.Y. Verbakel, E. Christodoulou, A.J. Vickers, et al., Reporting and interpreting decision curve analysis: a guide for investigators, Eur. Urol. 74 (6) (2018) 796–804, doi:10.1016/j.eururo.2018.08.038.
[23] Y.R. Miao, Q. Zhang, Q. Lei, M. Luo, G.Y. Xie, H. Wang, et al., ImmuCellAI: a unique method for comprehensive T-Cell subsets abundance prediction and its application in cancer immunotherapy, Adv. Sci. 7 (7) (2020) 1902880 (Weinh), doi:10.1002/advs.201902880.
[24] B. Zhang, S. Horvath, A general framework for weighted gene co-expression network analysis, Stat. Appl. Genet. Mol. Biol. 4 (2005) Article17, doi:10.2202/1544-6115.1128.
[25] M. Niemira, F. Collin, A. Szalkowska, A. Bielska, K. Chwialkowska, J. Reszec, et al., Molecular signature of subtypes of non-small-cell lung cancer by large-scale transcriptional profiling: identification of key modules and genes by weighted gene co-expression network analysis (WGCNA), Cancers 12 (1) (2019) (Basel), doi:10.3390/cancers12010037.
[26] S. Yepes, R. López, R.E. Andrade, P.A. Rodriguez-Urrego, L. López-Kleine, M.M. Torres, Co-expressed miRNAs in gastric adenocarcinoma, Genomics 108 (2) (2016) 93–101, doi:10.1016/j.ygeno.2016.07.002.
[27] Z.S. Mustafin, S.A. Lashin, Y.G. Matushkin, K.V. Gunbin, Afonnikov DA, Orthoscape: a cytoscape application for grouping and visualization KEGG based gene networks by taxonomy and homology principles, BMC Bioinf. 18 (Suppl 1) (2017) 1427, doi:10.1186/s12859-016-1427-5.
[28] E.G. Shaw, B. Berkey, S.W. Coons, D. Bullard, D. Brachman, J.C. Buckner, et al., Recurrence following neurosurgeon-determined gross-total resection of adult supratentorial low-grade glioma: results of a prospective clinical trial, J. Neurosurg. 109 (5) (2008) 835–841, doi:10.3171/JNS/2008/109/11/0835.
[29] F. Pignatti, M. van den Bent, D. Curran, C. Debruyne, R. Sylvester, P. Therasse, et al., Prognostic factors for survival in adult patients with cerebral low-grade glioma, J. Clin. Oncol. 20 (8) (2002) 2076–2084, doi:10.1200/JCO.2002.08.121.
[30] X. Zhou, S. Qiu, Di Jin, K. Jin, X. Zheng, L. Yang, Development and validation of an individualized immune-related gene pairs prognostic signature in papillary renal cell carcinoma, Front. Genet. 11 (2020) 569884, doi:10.3389/fgene.2020.569884.
[31] P. Jiang, Y. Li, Z. Xu, S. He, A signature of 17 immune-related gene pairs predicts prognosis and immune status in HNSCC patients, Transl. Oncol. 14 (1) (2021) 100924, doi:10.1016/j.tranon.2020.100924.
[32] B. Li, Y. Cui, M. Diehn, R. Li, Development and validation of an individualized immune prognostic signature in early-stage nonsquamous non-small cell lung cancer, JAMA Oncol. 3 (11) (2017) 1529–1537, doi:10.1001/jamaoncol.2017.1609.
[33] J. Wu, Y. Zhao, J. Zhang, Q. Wu, W. Wang, Development and validation of an immune-related gene pairs signature in colorectal cancer, Oncoimmunology 8 (7) (2019) 1596715, doi:10.1080/2162402X.2019.1596715.
[34] M. Zhang, X. Wang, X. Chen, Q. Zhang, J. Hong, Novel immune-related gene signature for risk stratification and prognosis of survival in lower-grade glioma, Front. Genet. 11 (2020) 363, doi:10.3389/fgene.2020.00363.
[35] W. Cheng, X. Ren, C. Zhang, J. Cai, Y. Liu, S. Han, et al., Bioinformatic profiling identifies an immune-related risk signature for glioblastoma, Neurology 86 (24) (2016) 2226–2234, doi:10.1212/WNL.0000000000002770.
[36] P. Chuntova, K.M. Downey, B. Hegde, N.D. Almeida, H. Okada, Genetically engineered T-Cells for malignant glioma: overcoming the barriers to effective immunotherapy, Front. Immunol. 9 (2018) 3062, doi:10.3389/fimmu.2018.03062.
[37] J. Wei, A. Marisetty, B. Schrand, K. Gabrusiewicz, Y. Hashimoto, M. Ott, et al., Osteopontin mediates glioblastoma-associated macrophage infiltration and is a potential therapeutic target, J. Clin. Invest. 129 (1) (2019) 137–149, doi:10.1172/JCI121266.
[38] S.T. Schafer, A.C.M. Paquola, S. Stern, D. Gosselin, M. Ku, M. Pena, et al., Pathological priming causes developmental gene network heterochronicity in autistic subject-derived neurons, Nat. Neurosci. 22 (2) (2019) 243–255, doi:10.1038/s41593-018-0295-x.
[39] S. Han, C. Zhang, Q. Li, J. Dong, Y. Liu, Y. Huang, et al., Tumor-infiltrating CD4(+) and CD8(+) lymphocytes as predictors of clinical outcome in glioma, Br. J. Cancer 110 (10) (2014) 2560–2568, doi:10.1038/bjc.2014.162.
[40] L. Mu, C. Yang, Q. Gao, Y. Long, H. Ge, G. DeLeon, et al., CD4+ and perivascular Foxp3+ T cells in glioma correlate with angiogenesis and tumor progression, Front. Immunol. 8 (2017) 1451, doi:10.3389/fimmu.2017.01451.
[41] E. Chai, L. Zhang, C. Li, LOX-1+ PMN-MDSC enhances immune suppression which promotes glioblastoma multiforme progression, Cancer Manag. Res. 11 (2019) 7307–7315, doi:10.2147/CMAR.S210545.
[42] A.L. Hung, R. Maxwell, D. Theodros, Z. Belcaid, D. Mathios, A.S. Luksik, et al., TIGIT and PD-1 dual checkpoint blockade enhances antitumor immunity and survival in GBM, Oncoimmunology 7 (8) (2018) e1466769, doi:10.1080/2162402X.2018.1466769.
[43] S. Liu, Z. Wang, Y. Wang, X. Fan, C. Zhang, W. Ma, et al., PD-1 related transcriptome profile and clinical outcome in diffuse gliomas, Oncoimmunology 7 (2) (2018) e1382792, doi:10.1080/2162402X.2017.1382792.
[44] L. Peng, Z. Chen, Y. Chen, X. Wang, N. Tang, MIR155HG is a prognostic biomarker and associated with immune infiltration and immune checkpoint molecules expression in multiple cancers, Cancer Med. 8 (17) (2019) 7161–7173, doi:10.1002/cam4.2583.

[45] S. Koyama, E.A. Akbay, Y.Y. Li, G.S. Herter-Sprie, K.A. Buczkowski, W.G. Richards, et al., Adaptive resistance to therapeutic PD-1 blockade is associated with upregulation of alternative immune checkpoints, Nat. Commun. 10501 (2016), doi:10.1038/ncomms10501.

[46] S. Qin, L. Xu, M. Yi, S. Yu, K. Wu, S. Luo, Novel immune checkpoint targets: moving beyond PD-1 and CTLA-4, Mol. Cancer 155 (2019), doi:10.1186/s12943-019-1091-2.

[47] L. Tu, R. Guan, H. Yang, Y. Zhou, W. Hong, L. Ma, et al., Assessment of the expression of the immune checkpoint molecules PD-1, CTLA4, TIM-3 and LAG-3 across different cancers in relation to treatment response, tumor-infiltrating immune cells and survival, Int. J. Cancer (2020) 423–439, doi:10.1002/ijc.32785.

[48] C. Zou, C. Zhu, G. Guan, Q. Guo, T. Liu, S. Shen, et al., CD48 is a key molecule of immunomodulation affecting prognosis in glioma, OncoTargets Ther. (2019) 4181–4193, doi:10.2147/OTT.S198762.